

# Effectiveness of piezoelectric fiber reinforced composite laminate in active damping for smart structures

Ravindra Singh Chahar<sup>1</sup> and Ravi Kumar B.\*<sup>2</sup>

<sup>1</sup> Department of Aeronautical Engineering, Manav Rachna International Institute of Research & Studies, Faridabad, Haryana 121002, India  
<sup>2</sup> School of Mechanical Engineering, SASTRA Deemed University, Thanjavur, Tamilnadu 613402, India

(Received January 14, 2019, Revised March 6, 2019, Accepted March 23, 2019)

**Abstract.** This paper deals with the effect of ply orientation and control gain on tip transverse displacement of functionally graded beam layer for both active constrained layer damping (ACLD) and passive constrained layer damping (PCLD) system. The functionally graded beam is taken as host beam with a bonded viscoelastic layer in ACLD beam system. Piezoelectric fiber reinforced composite (PFRC) laminate is a constraining layer which acts as actuator through the velocity feedback control system. A finite element model has been developed to study actuation of the smart beam system. Fractional order derivative constitutive model is used for the viscoelastic constitutive equation. The control voltage required for ACLD treatment for various symmetric ply stacking sequences is highest in case of longitudinal orientation of fibers of PFRC laminate over other ply stacking sequences. Performance of symmetric and anti-symmetric ply laminates on damping characteristics has been investigated for smart beam system using time and frequency response plots. Symmetric and anti-symmetric ply laminates significantly reduce the amplitude of the vibration over the longitudinal orientation of fibers of PFRC laminate. The analysis reveals that the PFRC laminate can be used effectively for developing very light weight smart structures.

**Keywords:** finite element model; control gain; ACLD; PCLD; functionally graded beam; PFRC

## 1. Introduction

The demand for new generation of advanced materials in modern industrial applications has led to the development of the smart materials. The idea of smart materials originated in the mid-1980s (Tzou *et al.* 2004). Their characteristics are an ability to be clever, active, and sophisticated. Examples of smart materials include a piezoelectric material, an electrostrictive material, a magnetostrictive material, shape memory alloys, and optical fibers. Active vibration damping, energy harvesting, and structural health monitoring are some of the applications of piezoelectric materials. In piezoelectric materials, mechanical energy can be converted to electrical energy and vice versa at frequency ranges which are required for technical applications such as vibration damping.

Light weight structures require integration of active means of control to tackle the problems of low inherent damping and large vibrations. Suitable use of piezoelectric fiber reinforced composites (PFRCs) has been done for such applications (Xiong and Tian 2017). PFRCs can be utilized as distributed sensors and actuators to monitor the health of the structure. Functionally graded materials consist of two or more material components whose relative volume fractions and microstructures are engineered to have gradually varying properties. Abrupt change in material properties can result in delamination due to large inter-

aminar stresses, and the initiation followed by propagation of cracks due to large plastic deformation at the interfaces. The viscoelastic layer is considered passive due to its inability to respond to the system. It is subjected to both direct and shear strain caused by its damping layer, resulting in energy dissipation. (Kumar and Ray 2012) examined that vertical orientation of fibers can be utilized for tuning of thickness mode of vibrations. This kind of arrangement of fibers in composites can be used as transducers. (Polit *et al.* 2016) developed eight noded finite elements using C0 approximations. The interpolation function used for transverse displacement was quadratic. For the piezoelectric approximation, a layer-wise description is used with a cubic variation in the thickness of each layer while the potential is assumed to be constant on each elementary domain for the in-plane variation. They developed the finite element for both thick and thin plates without any shear or thickness locking problem.

Bekuit *et al.* (2009) developed quasi-2D finite element formulation for active-constrained layer beams. Passive damping in the system was provided by a viscoelastic layer, and a piezoelectric actuation layer was used to achieve active damping. (Galucio *et al.* 2004) investigated finite element formulation of viscoelastic sandwich beams using fractional derivative operators. (Ray and Mallik 2004) investigated the bending mode of actuation where piezoelectric fibers were oriented longitudinally. The performance of laminated composite beams having active constrained layer damping treatment was investigated in which constraining layer was made of piezoelectric fiber reinforced composite. (Yuvaraja and Senthilkumar 2013)

\*Corresponding author, Professor,  
E-mail: [ravikumar@mech.sastra.edu](mailto:ravikumar@mech.sastra.edu)

presented a comparative study on vibration characteristics of a flexible GFRP composite beam using SMA and PZT actuators. In the former case, GFRP beam modeled in cantilevered configuration with externally attached SMAs. In the later case, GFRP beam with surface bonded PZT patches is analyzed for its vibration characteristics. They carried out experimental work for both cases in order to evaluate the vibration control of flexible beam for the first mode, also to find the effectiveness of the proposed actuators and verified numerically. As a result, the vibration characteristic of GFRP beam was more effective when SMA is used as an actuator.

Mohammadimehr *et al.* (2018) carried out bending, buckling and free vibration of CNT reinforced composites and presented a detailed method to analyze such a structure. (Ebrahimi and Barati 2016) carried out buckling analysis of embedded piezo-electro-magnetically actuated nanoscale beams and presented an exact mathematical solution to the governing differential equations. (Ebrahimi and Barati 2018) in another study analyzed Stability of functionally graded heterogeneous piezoelectric nanobeams based on nonlocal elasticity theory and presented a detailed method to analyze such a system. (Akbaş 2018) carried out forced vibration analysis of cracked functionally graded microbeams. (Aydogdu 2014) presented a study on the vibration of aligned carbon nanotube reinforced composite beams and showed the effect of nanotubes alignments on the mechanical properties of composite beams. (Panda *et al.* 2016) carried out a study on active vibration control of smart functionally graded beams. This work was devoted to examine the performance of the constraining layer of the active constrained layer damping (ACLD) treatment made of the active fiber composites (AFC) materials for vibration control of functionally graded (FG) beams. Finite Element (FE) model was developed to describe the open loop and closed loop dynamics of the FG beams integrated with the patches of the ACLD treatment. The closed loop frequency response functions computed by the FE models revealed that the ACLD treatment with its constraining layer composed of AFC material significantly enhances the damping characteristics of the FG beams. (Kumar and Ray 2012) presented a detailed study on active constrained layer damping of smart laminated composite sandwich plates using 1–3 piezoelectric composites.

Kanasogi and Ray (2013) carried out a study on active constrained layer damping of smart skew laminated composite plates using 1–3 piezoelectric composites. A finite element model was developed for accomplishing the task of the active constrained layer damping of skew laminated symmetric and anti-symmetric cross-ply and anti-symmetric angle-ply composite plates integrated with the patches of such ACLD treatment. Both in-plane and out-of-plane actuation by the constraining layer of the ACLD treatment were utilized for deriving the finite element model. The analysis revealed that the vertical actuation dominates over the in-plane actuation. Recently, (Panda and Kumar 2018) presented a detailed study on the design of active constrained layer damping treatment for vibration control of circular cylindrical shell structure.

A new 1-3 viscoelastic composite material (VECM)

layer was designed for improved active constrained layer damping (ACLD) treatment of vibration of a functionally graded (FG) circular cylindrical shell. Besides this improved active damping treatment, another objective of this study was to control all the modes of vibration of the shell effectively using the treatment (active constrained layer damping) in layer-form throughout the outer shell-surface. (Datta and Ray 2018) reported a study on smart damping of geometrically nonlinear vibrations of composite shells using fractional order derivative viscoelastic constitutive relations and presented a detailed method of analyzing such structures. (Nguyen-Quang *et al.* 2018) reported a study on an iso-geometric approach for the dynamic response of laminated FG-CNT reinforced composite plates integrated with piezoelectric layers. This study proposed an extension of the iso-geometric approach for the dynamic response of laminated carbon nanotube reinforced composite (CNTRC) plates integrated with piezoelectric layers. The mechanical displacement field is approximated according to the higher-order shear deformation theory (HSDT) using the formulation based on non-uniform rational B-spline (NURBS) basis functions. (Sheng and Wang 2009) presented a study on active control of functionally graded laminated cylindrical shells and proposed an analytical method on active vibration control of smart FG laminated cylindrical shells with thin piezoelectric layers based on Hamilton's principle. The thin piezoelectric layers embedded on inner and outer surfaces of the smart FG laminated cylindrical shell act as distributed sensor and actuator, which are used to control vibration of the smart FG laminated cylindrical shell under thermal and mechanical loads.

Various studies on active constrained layer damping and its analysis methods are reported in the literature (Ghashochi-Bargh and Sadr 2014, Li *et al.* 2016, Bendine *et al.* 2016, Cortés and Sarría 2015, Khalfi and Ross 2013, Edery-Azulay and Abramovich 2006, Sheng and Wang 2009, Kumar 2018, Su *et al.* 2016, Benbakhti *et al.* 2016, Zemirline *et al.* 2015, Kumar and Deol 2017).

The objective of the present work deals with the effect of ply orientation and control gain on tip transverse displacement of functionally graded beam layer for both active constrained layer damping (ACLD) and passive constrained layer damping (PCLD) system. The functionally graded beam is considered as host beam with

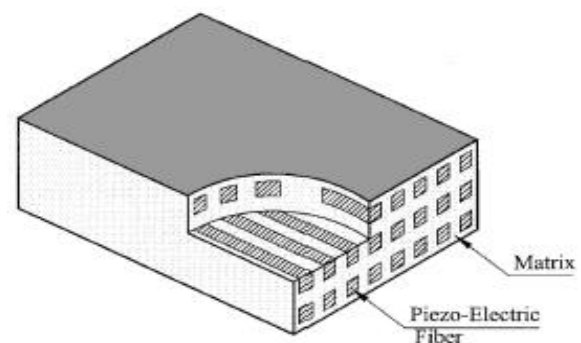


Fig. 1 Schematic diagram of a PFRC lamina

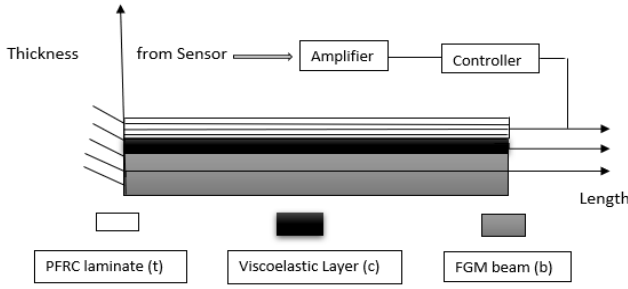


Fig 2 Schematic diagram of a composite beam integrated with ACLD treatment

a bonded viscoelastic layer in ACLD beam system. Piezoelectric fiber reinforced composite (PFRC) laminate is a constraining layer which acts as actuator through the velocity feedback control system. A finite element model has been developed to study the actuation of the smart beam system. Fig. 1 shows the piezoelectric fiber reinforced composite.

It has been examined that the control gain increases, the amplitude of the vibration reduce significantly. In this paper, a three-layered composite beam as shown in Fig. 2 is analyzed. The host beam is a functionally graded material (FGM) with through the thickness varying material properties (Young's modulus, Poisson's ratio, and density). The FGM is bonded to a viscoelastic material which on the other side is bonded to the PFRC laminate layer. Fig. 2 is a schematic of the ACLD beam system where a sensor measures the tip velocity, which is then fed through the controller to obtain a voltage that is applied to the PFRC laminate. The bottom layer is denoted by  $b$ , the viscoelastic layer is denoted by  $c$  and PFRC laminate is denoted by  $t$ . The PFRC laminate acts as an actuator and the applied voltage is the output of a constant gain velocity feedback control.

## 2. Mathematical modelling

### 2.1 Kinematic and constitutive relation

Timoshenko beam theory is used for approximation of displacement field for bottom FGM layer. The FGM beam has an axial displacement that is linearly interpolated across the beam thickness and a through-the-thickness independent transverse displacement represented by  $\{\bar{u}_b\}$  and  $\{\bar{w}_b\}$ , respectively. The displacement vector of the FGM beam  $\{\bar{d}_b\}$  is written as

$$\{\bar{d}_b\} = \begin{Bmatrix} \bar{u}_b(x, z_b, t) \\ \bar{w}_b(x, z_b, t) \end{Bmatrix} = \begin{Bmatrix} u_b(x, t) - z_b \phi_b(x, t) \\ w_b(x, t) \end{Bmatrix} \quad (1)$$

Defining a new vector  $\{v_b^T\} = \{u \ w \ \phi\} \{u_b \ w_b \ \phi_b\}$  gives the following expression for  $\{\bar{d}_b\}$

$$\{\bar{d}_b\} = \begin{bmatrix} 1 & 0 & -z_b \\ 0 & 1 & 0 \end{bmatrix} \{u_b \ w_b \ \phi_b\}^T = [z_b] \{v_b\} \quad (2)$$

The strain-displacement relations are given as

$$\bar{q}_b = \begin{Bmatrix} \dot{q}_x(x, z_b, t) \\ \gamma_{zx}(x, z_b, t) \end{Bmatrix}_b = \begin{Bmatrix} \frac{\delta \bar{u}_b}{\delta x} \\ \frac{\delta \bar{u}_b}{\delta z_b} + \frac{\delta \bar{w}_b}{\delta x} \end{Bmatrix} \quad (3)$$

$$= \begin{bmatrix} 1 & -z_b & 0 & 0 \\ 0 & 0 & -1 & 1 \end{bmatrix} [D_b] \begin{Bmatrix} u_b \\ w_b \\ \phi_b \end{Bmatrix} \equiv [z_b] [D_b] \{v_b\}$$

Where the derivative operator matrix  $[D_b]$  is given as

$$[D_b] = \begin{bmatrix} \frac{\delta}{\delta x} & 0 & 0 \\ 0 & 0 & \frac{\delta}{\delta x} \\ 0 & 0 & 1 \\ 0 & \frac{\delta}{\delta x} & 0 \end{bmatrix} \quad (4)$$

The 2-dimensional stress-strain constitutive relations for orthotropic FGM where the principal material properties coincide with both  $x$  and  $z$ -axes are given as

$$\begin{Bmatrix} \sigma_x \\ \sigma_z \\ \tau_{xz} \end{Bmatrix}_b = \begin{bmatrix} c_{11}(z) & c_{13}(z) & 0 \\ c_{11}(z) & c_{33}(z) & 0 \\ 0 & 0 & c_{55}(z) \end{bmatrix} \begin{Bmatrix} \dot{q}_x \\ \dot{q}_z \\ \gamma_{xz} \end{Bmatrix}_b \quad (5)$$

Where  $\sigma_x$  and  $\sigma_z$  are the normal stresses in the  $x$  and  $z$  directions, respectively,  $\gamma_{xz}$  is the shear stress in the  $xz$  plane and  $c_{ij}$  are the elastic constants of the material. With the assumption that stress in the  $z$  direction is zero (i.e.,  $\sigma_z = 0$ ), then  $\epsilon_z = -\frac{c_{11}}{c_{33}} \epsilon_x$  and introducing  $\bar{c}_{11} = \left(c_{11} - \frac{c_{13}^2}{c_{33}}\right)$ , the reduced constitutive relation is written as

$$\bar{\sigma}_b = \begin{Bmatrix} \sigma_x \\ \tau_{xz} \end{Bmatrix}_b = \begin{bmatrix} \bar{c}_{11}(z) & 0 \\ 0 & c_{55}(z) \end{bmatrix} \begin{Bmatrix} \dot{q}_x \\ \gamma_{xz} \end{Bmatrix}_b \quad (6)$$

For viscoelastic layer, axial and transverse displacements are interpolated through the thickness by cubic and quadratic polynomial functions, respectively. The displacement vector  $\{\bar{d}_c\}$  is characterized as

$$\{\bar{d}_c\} = \begin{Bmatrix} \bar{u}_c(x, z_c, t) \\ \bar{w}_c(x, z_c, t) \end{Bmatrix} = \begin{Bmatrix} C_1(u_b(x, t) - h_b \phi_b(x, t)) + C_2 u_{c2} + C_3 u_{c3} + C_4(u_b(x, t) + h_b \phi_b(x, t)) \\ E_1 w_b(x, t) + E_2 w_c(x, t) + E_3 w_t(x, t) \end{Bmatrix} \quad (7)$$

Where  $u_{c2} = \bar{u}_c(x, z_c = -\frac{h_c}{3}, t)$ ,  $u_{c3} = \bar{u}_c(x, z_c = -hc3, t)$ .

$C_1, C_2, C_3, C_4, E_1, E_2$  and  $E_3$  are functions of  $h_c$  and  $z_c$ .

The relation is further expanded with a new vector  $\{v_c^T\} = \{u_b \ w_b \ \phi_b \ u_{c2} \ u_{c3} \ w_c \ u_t \ w_t \ \phi_t\}$  as

$$\{\bar{d}_c\} = \begin{bmatrix} C_1 & 0 & -h_b C_1 & C_2 & C_3 & 0 & C_4 & 0 & h_t C_4 \\ 0 & E_1 & 0 & 0 & 0 & E_2 & 0 & E_3 & 0 \end{bmatrix} \begin{Bmatrix} u_b \\ w_b \\ \phi_b \\ u_{c2} \\ u_{c3} \\ w_c \\ u_t \\ w_t \\ \phi_t \end{Bmatrix} \equiv [Z_c]\{v_c\} \quad (8)$$

The strain-displacement relations for the viscoelastic layer are given as

$$\bar{\epsilon}_c = \begin{Bmatrix} \epsilon_x \\ \epsilon_z \\ \gamma_{zx} \end{Bmatrix} = \begin{Bmatrix} \frac{\delta \bar{u}_c}{\delta x} \\ \frac{\delta \bar{w}_c}{\delta z_c} \\ \frac{\delta \bar{u}_c}{\delta z_c} + \frac{\delta \bar{w}_c}{\delta x} \end{Bmatrix} \quad (9)$$

The strain vector takes the following compact matrix form

$$\{\bar{d}_c\} = [\tilde{Z}_c][D_c] \begin{Bmatrix} u_b \\ w_b \\ \phi_b \\ u_{c2} \\ u_{c3} \\ w_c \\ u_t \\ w_t \\ \phi_t \end{Bmatrix} \equiv [\tilde{Z}_c][D_c] \{v_c\}$$

Where  $\{\tilde{Z}_c\}$  matrix is given by  $\{\tilde{Z}_c\} = [[\tilde{Z}_{c1}] \ [\tilde{Z}_{c2}]]$ . and  $[D_c]$  is 18x9 a matrix.

Where

$$[\tilde{Z}_{c1}] = \begin{bmatrix} C_1 & -h_b C_1 & C_2 & C_3 & C_4 & h_t C_4 & 0 & 0 & 0 \\ 0 & 0 & 0 & 0 & 0 & 0 & \frac{\partial E_1}{\partial z_c} & \frac{\partial E_2}{\partial z_c} & \frac{\partial E_3}{\partial z_c} \\ 0 & 0 & 0 & 0 & 0 & 0 & 0 & 0 & 0 \end{bmatrix}$$

And

$$[\tilde{Z}_{c2}] = \begin{bmatrix} 0 & 0 & 0 & 0 & 0 & 0 & 0 & 0 & 0 \\ 0 & 0 & 0 & 0 & 0 & 0 & 0 & 0 & 0 \\ \frac{\partial C_1}{\partial z_c} & -h_b \frac{\partial C_1}{\partial z_c} & \frac{\partial C_2}{\partial z_c} & \frac{\partial C_3}{\partial z_c} & \frac{\partial C_4}{\partial z_c} & h_t \frac{\partial C_4}{\partial z_c} & E_1 & E_2 & E_3 \end{bmatrix}$$

The constitutive relation can be mathematically written

as (Galucio *et al.* 2004)

$$\bar{\sigma}_c(t) + \tau^\alpha \frac{d^\alpha \bar{\sigma}_c(t)}{dt^\alpha} = E_0 [\xi_c] \bar{q}_c(t) + \tau^\alpha E_\infty [\xi_c] \frac{d^\alpha \bar{q}_c(t)}{dt^\alpha} \quad (10)$$

Where  $[\xi_c]$  is a matrix given by the following relation:

The two-dimensional stress-strain constitutive relation is  $\{\sigma\}_c \equiv [Q_c] \bar{O}_c$ , where  $[Q_c]$  is elasticity matrix. Under plain strain condition, the elasticity matrix is given as follows

$$[Q_c] = E_c [\xi_c],$$

Where

$$[\xi_c] = \frac{1}{(1+\nu_c)(1-2\nu_c)} \begin{bmatrix} 1-\nu_c & \nu_c & 0 \\ \nu_c & 1-\nu_c & 0 \\ 0 & 0 & (1-2\nu_c)/2 \end{bmatrix},$$

$E_0, E_\infty$  are relaxed and non-relaxed elastic moduli,  $\tau$  is the relaxation time, and  $\alpha$  is the fractional derivative order ( $0 < \alpha < 1$ ).

The fractional operator  $\frac{d^\alpha}{dt^\alpha}$  is approximated by the Grünwald definition by finite difference as

$$\frac{d^\alpha f(t)}{dt^\alpha} \approx \square t^{-\alpha} \sum_{j=0}^{N_t} A_{j+1} f(t-j\square t) \quad (11)$$

Where  $\square t = \frac{t}{N}$  is the time step increment,  $N_t$  is the total number of terms where  $N_t < N$ , and  $A_{j+1}$  are the Grünwald coefficients given by the recurrence formula

$$A_{j+1} = \frac{j-\alpha-1}{j} A_j = \prod_{p=1}^j \frac{p-\alpha-1}{p}$$

Defining a new vector  $\{v_c^T\} = [N_t]q_e$ ,  $\{u_t^T\} = \{u_t \ w_t \ \phi_t\}$  gives the following expression for  $\{\bar{d}_t\}$

$$\{\bar{d}_t\} = \begin{bmatrix} 1 & 0 & -z_t \\ 0 & 1 & 0 \end{bmatrix} \{u_t \ w_t \ \phi_t\}^T = [z_t] \{v_t\}$$

The strain-displacement relations for the top layer are given as

$$\bar{q} = \begin{Bmatrix} \dot{q}_x(x, z_t, t) \\ \gamma_{zx}(x, z_t, t) \end{Bmatrix}_t = \begin{Bmatrix} \frac{\delta \bar{u}_t}{\delta x} \\ \frac{\delta \bar{u}_t}{\delta z_t} + \frac{\delta \bar{w}_t}{\delta x} \end{Bmatrix}$$

The strain vector  $\bar{O}$  can be written in the following form as

$$\bar{q} = \begin{Bmatrix} \dot{q}_x \\ \gamma_{zx} \end{Bmatrix}_t = \begin{Bmatrix} \frac{\delta u_t}{\delta x}(x, t) \\ -\phi_t(x, t) + \frac{\delta w_t}{\delta x}(x, t) \end{Bmatrix}_t - z_t \begin{Bmatrix} \frac{\delta \phi_t}{\delta x}(x, t) \\ 0 \end{Bmatrix}_t = \begin{Bmatrix} \dot{q}_x^0 \\ \gamma_{zx}^0 \end{Bmatrix}_t + z_t \begin{Bmatrix} k_x \\ k_{xz} \end{Bmatrix}_t \equiv \dot{q}_0 + z_t k$$

Hence

$$\bar{Q} = [1 \ z_t] \begin{Bmatrix} \dot{Q}_0 \\ k \end{Bmatrix}_t = [1 \ z_t] \begin{bmatrix} D_t^0 \\ D_t^1 \end{bmatrix} \{v_t\} \quad (12)$$

Where the derivative operator matrices  $[D_t^0]$  and  $[D_t^1]$  are given as

$$[D_t^0] = \begin{bmatrix} \frac{\partial}{\partial x} & 0 & 0 \\ 0 & 0 & \frac{\partial}{\partial x} \end{bmatrix}, \quad [D_t^1] = \begin{bmatrix} 0 & \frac{\partial}{\partial x} & 1 \\ 0 & 0 & 0 \end{bmatrix}$$

The electric potential  $\Psi_t$  is assumed to vary linearly through the thickness of the piezoelectric layer and is expressed as

$$\Psi_t(x, z_t, t) = \Psi_0(x, t) + z_t \frac{\partial \Psi_t(x, z_t, t)}{\partial z_t} \quad (13)$$

Where  $\Psi_0$  and  $\frac{\partial \Psi_t}{\partial z_t}$  are the electric potential and its gradient at the mid-plane of the PFRC laminate, respectively? If the axial component of the electric field is neglected (i.e.,  $E_x = 0$ ) The electric potential can be differentiated with respect to the transverse coordinate to obtain the transverse electrical equation, which can be written as

$$E_z = -\frac{\partial \Psi_t}{\partial z_t} = \frac{V}{h_t} \quad (14)$$

Where  $V$  is the applied voltage and  $h_t$  is the PFRC laminate thickness.

Assuming that  $\sigma_y = \tau_{yz} = \tau_{xy} = 0$  albeit  $\dot{Q}_y \neq \gamma_{yz} \neq \gamma_{xy} \neq 0$ ,  $E_x = E_y = 0$  and noting that  $E_x = E_y = 0$  because the piezoelectric fibers are polarized only through the thickness, the constitutive equation is given by the following equation

$$\begin{aligned} \{\bar{\sigma}_t\}_k &= \begin{Bmatrix} \sigma_x \\ \tau_{xz} \end{Bmatrix}_k = \begin{bmatrix} \bar{Q}_{11} & 0 \\ 0 & k_s \bar{Q}_{55} \end{bmatrix} \begin{Bmatrix} \dot{Q}_x \\ \gamma_{xz} \end{Bmatrix}_k - \begin{Bmatrix} \bar{e}_{31} E_z \\ 0 \end{Bmatrix}_k \\ &\equiv [\bar{Q}_t]_k \{\dot{Q}\}_k - \begin{Bmatrix} \bar{e}_{31} E_z \\ 0 \end{Bmatrix}_k \end{aligned} \quad (15)$$

Where  $\bar{Q}_{ij}$ 's and  $\bar{e}_{31}$  are coefficients of elasticity and reduced piezoelectric constant as given in (Bekuit *et al.* 2009).

## 2.2 Variation of material properties across FGM

Depending on the application, the FGM beam may have its Young modulus, Poisson's ratio, and/or density varying continuously in the thickness direction, along with the z-axis (i.e.,  $E = E(z)$ ,  $\nu = \nu(z)$ ,  $\rho = \rho(z)$ ). The formulation for two types of volumes fraction methods: (1) power-law FGM (P-FGM); and (2) exponential FGM (E-FGM) may be written as:

- (1) In P-FGM the volume fraction is assumed to obey the power-law function

$$f(z) = \left( \frac{z+h}{2h} \right)^P$$

Where  $P$  is the material parameter and  $2h$  is the

thickness of the layer. The rule of the mixture is applied with the volume fraction  $f(z)$  to determine the effective material property.

$$G(z) = f(z)G_b^0 + [1 - f(z)]G_b^1$$

- (2) In E-FGM the volume fraction obeys the exponential function

$$G(z) = G_b^0 e^{\lambda(z+h)}$$

$$\text{With } \lambda = \frac{1}{2h} \ln \left( \frac{G_b^1}{G_b^0} \right)$$

Where  $G(z)$  represents any varying property (i.e.,  $G(z) = E = E(z)$ ,  $G(z) = \nu = \nu(z)$ , or  $G(z) = \rho = \rho(z)$ )

$G_b^0$  and  $G_b^1$  represent the corresponding material properties at the bottom and the top surfaces of the FGM beam, respectively, and  $\lambda$  is a parameter that describes the inhomogeneity of the FGM beam throughout the thickness.

## 2.3 Finite element modeling

There are five locations which have been selected to define the variations of displacements through the thickness of the system: one location is for the bottom FGM beam, three locations for the viscoelastic core, and one location for the top PFRC layer. The field variables for each layer are captured using these five locations. The quadratic interpolation of the transverse displacement field variables has been allowed using three nodes along the span of the beam as per Timoshenko's beam theory. Nodes 1 and 3 have the five locations for through the thickness displacements, while node 2 has the transverse displacement of each layer. The global displacement vector of an element can be written as

$$u_e^T = \{u_b \ w_b \ \phi_b \ u_{c2} \ u_{c3} \ w_c \ u_t \ w_t \ \phi_t\} \quad (16)$$

Where  $u_i$  and  $w_i$  are the axial and transverse displacement magnitudes, respectively, evaluated at  $i = b, c$  and  $t$  for the bottom, core and top layers, respectively. Also  $u_{c2}$  and  $u_{c3}$  are the two intermediate nodes in the core thickness.

First and third node each contains 9 degrees of freedom, and the middle node has 3 DOF, resulting in a total elemental DOF of 21. The element displacement vector  $q_e$  can be expressed as

$$\begin{aligned} q_e^T &= \{u_{b1} \ w_{b1} \ \phi_{b1} \ u_{c2,1} \ u_{c3,1} \ w_{c1} \ u_{t1} \ w_{t1} \ \phi_{t1} \ \dots \\ &\dots w_{b2} \ w_{c2} \ w_{t2} \ \dots \\ &\dots u_{b3} \ w_{b3} \ \phi_{b3} \ u_{c2,3} \ u_{c3,3} \ w_{c3} \ u_{t3} \ w_{t3} \ \phi_{t3}\} \end{aligned} \quad (17)$$

Where the subscripts  $b_j$ ,  $c_j$ , and  $t_j$  represents the bottom, core, and top layer, respectively with  $j = 1 \dots 3$  signifying the node numbers. A schematic diagram of a finite element of the system is given in Fig. 3. The axial displacement  $u$  and slope  $\phi$  field variables are interpolated along the span of the structure by a linear function, and transverse displacement field variable  $w$  by a quadratic function. These are:





Table 1 Constraining layer (PZT5H/EPOXY) properties

$C_{11}$ (GPa)	$C_{12}$ (GPa)	$C_{22}$ (GPa)	$C_{44}$ (GPa)	$C_{55}$ (GPa)	$e_{31}$ (C/m <sup>2</sup> )	$d_{33}$ (F/m)	$\rho$ (Kg/m <sup>3</sup> )
32.6	4.3	7.2	1.05	1.29	6.76	10.64*10 <sup>-9</sup>	3640

Table 2 Viscoelastic Core (ISD112) properties

$E_0$ (MPa)	$E_\infty$ (MPa)	$\nu$	$\rho$ (Kg/m <sup>3</sup> )
1.5	69.9495	0.5	1600

Table 3 FGM Host Beam ( $p = 0.66$  for power law) properties

Materials	$E$ (GPa)	$\nu$	$\rho$ (Kg/m <sup>3</sup> )
Aluminum	100	0.3	2700
Zirconia	352	0.3	5700

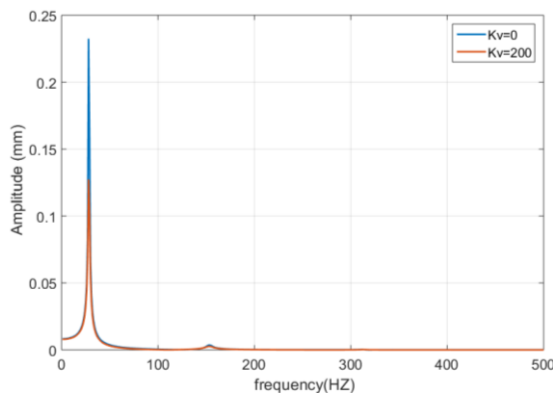


Fig. 4 Frequency response of active and passive damping (ACLD ( $K_v = 200$ )) at [0/0/0/0] degree ply stacking sequence

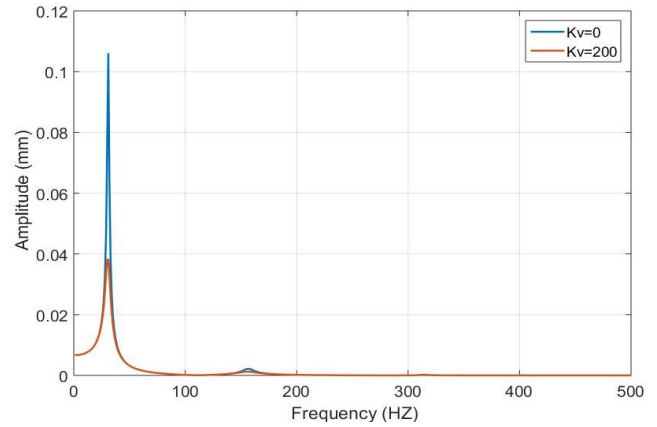
Result clearly reveals that the PFRC laminate significantly reduces the amplitude of vibrations, enhancing the damping characteristics of the system over the passive damping.

From Fig. 5(a), we observe that [45/-45/-45/45] degree stacking sequence gives better damping results than the longitudinal orientation of fibers of PFRC laminate given in Fig. 4 for both controlled and uncontrolled cases. Also, the maximum amplitude at  $K_v = 200$  is limited below 0.04 mm.

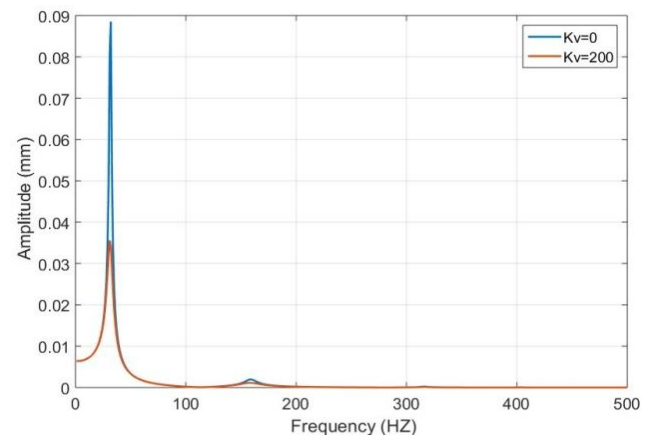
Fig. 5(b) shows the frequency response of active and passive damping ( $K_v = 200$ ) vs PCLD ( $K_v = 0$ ) for anti-symmetric ply laminate at [45/-45/45/-45] degree ply stacking sequence.

It can be seen that the anti-symmetric ply laminate gives better damping characteristics than symmetric ply laminate and significantly reduces the amplitude of the vibration of the beam system.

Time response (on x-axis) plot shown in Fig. 6 shows the vibration damping for various ply stacking sequences. It can be seen that the symmetric ply laminate at [45/-45/45/-45] degree ply stacking sequence significantly reduces the amplitude of the vibration. Ply laminate at [0/60/60/0] even though in symmetrical arrangement shows worst vibration



(a) Symmetric ply at [45/-45/-45/45] stacking sequence



(b) Anti-symmetric ply laminate at [45/-45/45/-45] stacking sequence

Fig. 5 Frequency response of active and passive damping (ACLD ( $K_v = 200$ ) vs PCLD ( $K_v = 0$ )) ply laminate

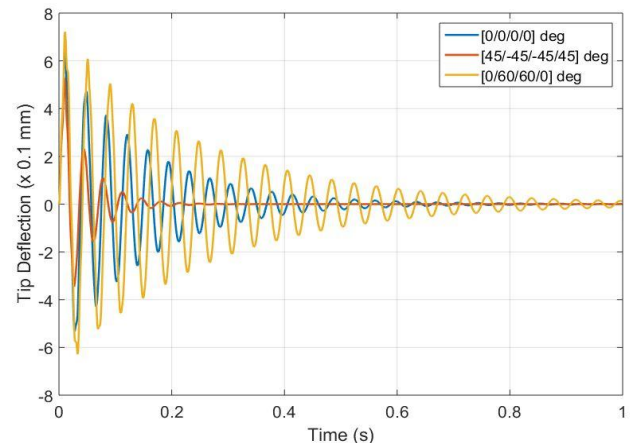


Fig. 6 Effect of stacking sequence on tip transverse displacement for controlled active damping ( $K_v = 350V/(m/s)$ ) for a fully clamped cantilever beam

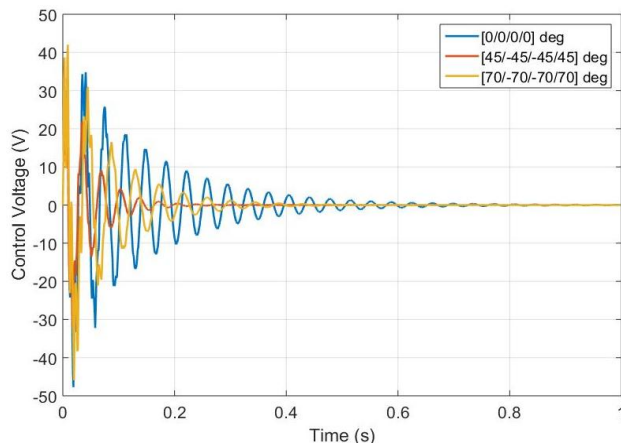


Fig. 7 Control voltage required for ACLD treatment for different ply stacking sequences ( $K_v = 350$  V/m/s)

damping characteristics. Ply laminate at [0/0/0/0] sequence shows an intermediate response to the vibration damping.

It can be seen in Fig. 7 that the control voltage required is maximum if fibers are oriented longitudinally for symmetric ply laminates and required voltage is minimum if fibers are oriented at [45/-45/45/-45] degree ply stacking sequence. The gain that is chosen to best represent the effects of the beam vibration is  $K_v = 350$  V/(m/s) for PFRCs. This gain is suitable since the resulting actuation voltage is not in the breakdown voltage range. Symmetric and anti-symmetric ply laminates significantly reduce the amplitude of the vibration over the longitudinal orientation of fibers of PFRC laminate.

#### 4. Conclusions

A finite element model has been developed to investigate the actuation of PFRC laminate of the cantilever beam coupled with ACLD treatment. The PFRC laminate acts as the actuator of the system through a velocity feedback control system. Fractional order derivative constitutive model is used for the viscoelastic constitutive equation. Time response and frequency response of the beam shows that PFRC laminate acting as actuator significantly enhances the damping characteristics of the beam system. Time and frequency response plots show that antisymmetric ply laminate gives better damping characteristics than symmetric ply laminate for beam system. The variation of control gain significantly affects the amplitude of the vibration. The gain that is chosen to best represent the effects of the beam vibration is  $K_v = 350$  V/(m/s) for PFRCs. This gain is suitable since the resulting actuation voltage is not in the breakdown voltage range, typically about 200 volts for most piezoelectric ceramics. Active constrained layer damping treatment shows better damping characteristics than passive controlled layer damping treatment. PFRC laminate can be used effectively for developing very lightweight smart structures possible applications in Aircraft and Automobile Industries.

#### References

- Akbaş, Ş.D. (2018), "Forced vibration analysis of cracked functionally graded microbeams", *Adv. Nano Res., Int. J.*, **6**(1), 39-55. DOI: 10.12989/ANR.2018.6.1.039
- Aydogdu, M. (2014), "On the vibration of aligned carbon nanotube reinforced composite beams", *Adv. Nano Res., Int. J.*, **2**(4), 199-210. DOI: 10.12989/anr.2014.2.4.199
- Bekuit, J.R., Oguamanam, D.C.D. and Damisa, O. (2009), "Quasi-2D finite element formulation of active-constrained layer beams", *Smart Mater. Struct.*, **18**(9), 095003. DOI: 10.1088/0964-1726/18/9/095003
- Benbakhti, A., Bouiadjra, M.B., Retiel, N. and Tounsi, A. (2016), "A new five unknown quasi-3D type HSDT for thermomechanical bending analysis of FGM sandwich plates", *Steel Compos. Struct., Int. J.*, **22**(5), 975-999. DOI: 10.12989/scs.2016.22.5.975
- Bendine, K., Boukhoulda, F.B., Nouari, M. and Satla, Z. (2016), "Active vibration control of functionally graded beams with piezoelectric layers based on higher order shear deformation theory", *Earthq. Eng. Eng. Vib.*, **15**(4), 611-620. DOI: 10.1007/s11803-016-0352-y
- Cortés, F. and Sarría, I. (2015), "Dynamic analysis of three-layer sandwich beams with thick viscoelastic damping core for finite element applications", *Shock Vib.*, 1-9. DOI: 10.1155/2015/736256
- Datta, P. and Ray, M.C. (2018), "Smart damping of geometrically nonlinear vibrations of composite shells using fractional order derivative viscoelastic constitutive relations", *Mech. Adv. Mater. Struct.*, **25**(1), 62-78. DOI: 10.1080/15376494.2016.1255811
- Ebrahimi, F. and Barati, M.R. (2016), "An exact solution for buckling analysis of embedded piezoelectro-magnetically actuated nanoscale beams", *Adv. Nano Res., Int. J.*, **4**(2), 65-84. DOI: 10.12989/anr.2016.4.2.065
- Ebrahimi, F. and Barati, M.R. (2018), "Stability analysis of functionally graded heterogeneous piezoelectric nanobeams based on nonlocal elasticity theory", *Adv. Nano Res., Int. J.*, **6**(2), 93-112. DOI: 10.12989/ANR.2018.6.2.093
- Ederly-Azulay, L. and Abramovich, H. (2006), "Augmented damping of a piezo-composite beam using extension and shear piezoceramic transducers", *Compos. Part B: Eng.*, **37**(4-5), 320-327. DOI: 10.1016/J.COMPOSITESB.2005.11.004
- Galucio, A.C., Deü, J.F. and Ohayon, R. (2004), "Finite element formulation of viscoelastic sandwich beams using fractional derivative operators", *Computat0 Mech.*, **33**, 282-291. DOI: 10.1007/s00466-003-0529-x
- Ghashochi-Bargh, H. and Sadr, M.H. (2014), "Vibration reduction of composite plates by piezoelectric patches using a modified artificial bee colony algorithm", *Latin Am. J. Solids Struct.*, **11**(10), 1846-1863. DOI: 10.1590/S1679-78252014001000009
- Kanasogi, R.M. and Ray, M.C. (2013), "Active constrained layer damping of smart skew laminated composite plates using 1-3 piezoelectric composites", *J. Compos.*, 1-17. DOI: 10.1155/2013/824163
- Khalfi, B. and Ross, A. (2013), "Influence of partial constrained layer damping on the bending wave propagation in an impacted viscoelastic sandwich", *Int. J. Solids Struct.*, **50**(25-26), 4133-4144. DOI: 10.1016/J.IJSOLSTR.2013.07.023
- Kumar, B.R. (2018), "Investigation on mechanical vibration of double-walled carbon nanotubes with inter-tube Van der waals forces", *Adv. Nano Res., Int. J.*, **6**(2), 135-145. DOI: 10.12989/anr.2018.6.2.135
- Kumar, B.R. and Deol, S. (2017), "Free Vibration Analysis of Double-Walled Carbon Nanotubes Embedded in an Elastic Medium Using DTM (Differential Transformation Method)", *J. Eng. Sci. Technol.*, **12**(10), 2700-2710.

- Kumar, R.S. and Ray, M.C. (2012), "Active constrained layer damping of smart laminated composite sandwich plates using 1–3 piezoelectric composites", *Int. J. Mech. Mater. Des.*, **8**(3), 197-218. DOI: 10.1007/s10999-012-9186-6
- Li, J., Ma, Z., Wang, Z. and Narita, Y. (2016), "Random vibration control of laminated composite plates with piezoelectric fiber reinforced composites", *Acta Mechanica Solida Sinica*, **29**(3), 316-327. DOI: 10.1016/S0894-9166(16)30164-1
- Logan, D.L. (2012), *A First Course in the Finite Element Method*, (Fourth Edition), <http://www.nelson.com>.
- Mohammadimehr, M., Mohammadi-Dehabadi, A.A., Akhavan Alavi, S.M., Alambeigi, K., Bamdad, M., Yazdani, R. and Hanifehlou, S. (2018), "Bending, buckling, and free vibration analyses of carbon nanotube reinforced composite beams and experimental tensile test to obtain the mechanical properties of nanocomposite", *Steel Compos. Struct., Int. J.*, **29**(3), 405-422. DOI: 10.12989/SCS.2018.29.3.405
- Nguyen-Quang, K., Vo-Duy, T., Dang-Trung, H. and Nguyen-Thoi, T. (2018), "An isogeometric approach for dynamic response of laminated FG-CNT reinforced composite plates integrated with piezoelectric layers", *Comput. Methods Appl. Mech. Eng.*, **332**, 25-46. DOI: 10.1016/J.CMA.2017.12.010
- Panda, S. and Kumar, A. (2018), "A design of active constrained layer damping treatment for vibration control of circular cylindrical shell structure", *J. Vib. Control*, **24**(24), 5811-5841. DOI: 10.1177/1077546316670071
- Panda, R.K., Nayak, B. and Sarangi, S.K. (2016), "Active vibration control of smart functionally graded beams", *Procedia Eng.*, **144**, 551-559. DOI: 10.1016/J.PROENG.2016.05.041
- Polit, O., D'Ottavio, M. and Vidal, P. (2016), "High-order plate finite elements for smart structure analysis", *Compos. Struct.*, **151**, 81-90. DOI: 10.1016/j.compstruct.2016.01.092
- Ray, M.C. and Mallik, N. (2004), "Active control of laminated composite beams using a piezoelectric fiber reinforced composite layer", *Smart Mater. Struct.*, **13**(1), 146-152. DOI: 10.1088/0964-1726/13/1/016
- Sheng, G.G. and Wang, X. (2009), "Active control of functionally graded laminated cylindrical shells", *Compos. Struct.*, **90**(4), 448-457. DOI: 10.1016/J.COMPSTRUCT.2009.04.017
- Su, L., Li, X. and Wang, Y. (2016), "Experimental study and modelling of CFRP-confined damaged and undamaged square RC columns under cyclic loading", *Steel Compos. Struct., Int. J.*, **21**(2), 411-427. DOI: 10.12989/scs.2016.21.2.411
- Tzou, H.S., Lee, H.J. and Arnold, S.M. (2004), "Smart materials, precision sensors/actuators, smart structures, and structronic systems", *Mech. Adv. Mater. Struct.*, **11**(4-5), 367-393. DOI: 10.1080/15376490490451552
- Xiong, Q.L. and Tian, X. (2017), "Transient thermo-piezo-elastic responses of a functionally graded piezoelectric plate under thermal shock", *Steel Compos. Struct., Int. J.*, **25**(2), 187-196. DOI: 10.12989/SCS.2017.25.2.187
- Yuvaraja, M. and Senthilkumar, M. (2013), "Comparative study on vibration characteristics of a flexible GFRP composite beam using SMA and PZT actuators", *Procedia Eng.*, **64**, 571-581. DOI: 10.1016/J.PROENG.2013.09.132
- Zemirline, A., Ouali, M. and Mahieddine, A. (2015), "Dynamic behavior of piezoelectric bimorph beams with a delamination zone", *Steel Compos. Struct., Int. J.*, **19**(3), 759-776. DOI: 10.12989/scs.2015.19.3.759